Chin. J. Astron. Astrophys. Vol. 6 (2006), No. 2, 141–154
(*http://www.chjaa.org*)

Chinese Journal of
Astronomy and
Astrophysics

Concordance of Kinematics and Lensing of Elliptical Galaxies with WMAP Cosmology *

HongSheng Zhao[1,2] and Bo Qin[1]

[1] National Astronomical Observatories, Chinese Academy of Sciences, Beijing 100012;
[2] SUPA, University of St. Andrews, KY16 9SS, UK; *hz4@st-andrews.ac.uk*

Received 2005 August 18; accepted 2005 December 4

Abstract We explore degeneracies in strong lensing model so to make time delay data consistent with the WMAP (Wilkinson Microwave Anisotropy Probe) cosmology. Previous models using a singular isothermal lens often yield a time delay between the observed multiple images too small than the observed value if we "hardwire" the now widely quoted post-WMAP "high" value of the Hubble constant ($H_0 \sim 71 \pm 4\,\mathrm{km\ s^{-1}\ Mpc^{-1}}$). Alternatively, the lens density profile (star plus dark matter) is required to be locally steeper than r^{-2} (isothermal) profile near the Einstein radius (of the order 3 kpc) to fit the time delays; a naive extrapolation of a very steep profile to large radius would imply a lens halo with a scale length of the order only 3 kpc, too compact to be consistent with CDM. We explore more sophisticated, mathematically smooth, positive lens mass density profiles which are consistent with a large halo and the post-WMAP H_0. Thanks to the spherical monopole degeneracy, the "reshuffling" of the mass in a lens model does not affect the quality of the fit to the image positions, amplifications, and image time delays. Even better, unlike the better-known mass sheet degeneracy, the stellar mass-to-light and the H_0 value are not affected either. We apply this monopole degeneracy to the quadruple imaged time-delay system PG 1115+080. Finally we discuss the implications of the time delay data on the newly proposed relativistic MOND theory.

Key words: cosmological parameters — dark matter — distance scale — gravitational lensing

1 INTRODUCTION

Gravitational lensing is a powerful tool for probing dark matter and constraining the cosmological model of our universe (e.g., Schneider et al. 1992; Wu 1996; Bartelmann & Schneider 2001; Chen 2004a, b). While image-splitting lenses provide mathematically rigorous and accurate constraints on the dark matter halos of lens galaxies, this technique has suffered from two puzzling problems for decades: (a) the anomalously large image flux ratio of adjacent pairs of images for any smooth lens model and (b) the anomalously low Hubble constant to fit the time delays with isothermal or other simple parametric models of dark halo. The first problem has recently been turned into a bonus point for the ΛCDM cosmology, which predicts substructures and clumpy lensing potential

* Supported by the National Natural Science Foundation of China.

(Metcalf & Zhao 2002 and references therein). Is the second problem a real problem for the ΛCDM cosmology, or a hint to explore beyond the standard density profiles for the baryons and the halo in ellipticals? This is the subject of this paper.

Almost from its infancy lensing has been promoted as the geometrical distance ruler for the Hubble constant (Refsdal 1964), which became the major driver for monitoring quasar light curves for time delays, i.e., the length difference of the gravitationally bended light paths between two images of a background quasar. Gradually it becomes clear that the lens is far from being a point mass deflector, there is perhaps more to be learned about the structure of the lens itself (usually a $\sim L_*$ E/S0 galaxy at redshift ~ 0.5) than the universe. A reliable measure for H_0 has been hampered to some extent by intrinsic degeneracies, such as the mass-sheet degeneracy (Gorenstein, Shapiro & Falco 1988), in the lens model, unbreakable by the strong lensing data alone (Williams & Saha 2000; Saha 2000; Saha & Williams 2001; Zhao & Pronk 2001). So far predictions for H_0 are model-dependent, and confirmation of lens models must wait a few years until dynamical data (e.g., in Koopmans & Treu 2002) with sufficient spatial resolution are collected for a large sample of high redshift lenses. Before that, some confirmation can come from a reliable "local template" of the mass profile from the kinematics in nearby E/S0 galaxies. The recent surprising finding of baryon-domination in the inner five effective radii from the PNe data of Romanowsky et al. (2003), together with the lack of a CDM cusp in disk galaxies and dwarf galaxies (see Weinberg & Katz 2003), highlights our gaps of knowledge about the inner halo, which is the region for strong lensing images, and cautions against blindly applying standard profiles for light and dark matter in ellipticals to lenses at high redshifts.

In recent years cosmological parameters are constrained more and more precisely by lensing-independent methods, e.g., $h_0 \equiv H_0/100\,\mathrm{km\ s^{-1}\ Mpc^{-1}} = 0.71 \pm 0.04$ from the post-WMAP data (Spergel et al. 2003) with the only assumption of a ΛCDM flat cosmology. The post-WMAP h_0 value is also consistent with $h_0 = 0.72 \pm 0.08$ from the HST Key Project (Freedman et al. 2001). These are two independent predictions which are based on very different data and assumptions. *If we accept these recent developments and the widely adopted values for* h_0, it would be interesting to ask whether the lensing community should reverse the application of time delay and refocus on systematic uncertainties of the lens potential and use the post-WMAP H_0 as one additional stringent constraint on the lens convergence (i.e., density) at the Einstein radius. First we would like to understand whether the cosmological parameters from WMAP and the strong lensing data *could* be made consistent with each other in a plausible model of the dark matter halo of the lens; a plausible galaxy model should yield a circular velocity curve with a flatness consistent with kinematic data of nearby luminous galaxies and weak shear measurements of low redshift galaxies. Second we would like to understand the degeneracies in the lens halo models, whether the same strong lensing data and cosmological parameters can yield very different lens models.

It is well-known that isothermal models and other simple smooth models of dark matter halos of gravitational lenses often predict a dimensionless time delay $H_0\Delta t$ much too small. Fitting the observed time delays Δt with lens models with an extended halo or a flat-rotation curve tend to yield an $h_0 \sim 0.5$ (e.g., Kochanek 2002a), too small to be comfortable with the HST Key Project Hubble constant $h_0 = 0.72 \pm 0.08$ (Freedman et al. 2001) and the post-WMAP cosmology $h_0 = 0.71 \pm 0.04$ (Spergel et al. 2003). The lensing predicted h_0 values are in general model dependent. Using general power-law lens models, Zhao & Pronk (2001) and Wucknitz (2002) found $h_0 \sim 0.5(2-\alpha)$, where $\alpha - 1 = \frac{d\log V_{\rm cir}^2}{d\log r}$ is the power-law slope of the deflection curve (or circular velocity curve) of the lens $V_{\rm cir}^2(r)$ as a function of the angular radius r from the lens center. So a WMAP $h_0 \sim 0.71$ would mean $\alpha \sim 0.6$, a significantly falling circular velocity curve, somewhat between a flat curve where $\alpha \sim 1$ and the Keplerian curve of a point mass where $\alpha \sim 0$.

The problem of the lens circular velocity curve also manifests in a direct comparison with kinematic data irrespective of the expectations of CDM models. Recent progress in the sophistication of the dynamical modelling of the mass distributions of nearby E/S0 galaxies allows us to gain control over various degeneracies in the velocity space and the line of sight projection, and to derive a less model-dependent mass distribution. It appears that the circular velocity curves of a large sample of E/S0 galaxies are consistent with being nearly flat. The variation is only 10% between 0.2 to 2 effective radii R_e (Gerhard et al. 2001), i.e., $|\alpha - 1| \leq 0.1$. The E/S0 lens galaxies at high redshift should have a deflection/rotation curve that is flat to a similar extent within one Einstein radius unless galaxy potentials evolve strongly with redshift. Note that strong lensing probes the mass distribution in the regions of one Einstein radius $R_{\rm E} \sim 2R_e$, which overlaps nicely with the region $0 - 5R_e$ for kinematic tracers in nearby E/S0 galaxies (Romanowsky et al. 2003). The comparison between lensing-inferred circular velocity curve with kinematic data will become more direct once we can measure velocity dispersion profiles of the lens galaxy, a task observationally difficult but promising (Tonry 1998; Koopmans & Treu 2002).

There are many open questions about the lenses. For example, are the lensing data consistent with other observations? Are lens models consistent with CDM? Is the post-WMAP H_0 consistent with lensing time delays? Are the mass distributions derived from dynamics and lensing consistent? Are the circular velocity curves of lenses peculiar or very different from isothermal? What is the baryonic fraction in lenses? Can lensing data be fit by a baryonic $R^{1/4}$-law plus an NFW halo (Navarro et al. 1997)? Or are there additional structures (e.g. nuclear disks, rings) and substructures (e.g. satellites)? Is the dark matter density profile modified by baryons?

Here we discuss the role of the monopole degeneracy in strong lensing models in softening the H_0 problem for dark matter halos. We use PG 1115 as an example, which is one of the very few quadruple systems that have been thoroughly studied observationally for decades. It has both accurate time delay data and kinematic data, and the lens and its neighbouring galaxies are also resolved. By fixing the h_0 to 0.71 we break the mass sheet degeneracy as well.

Our aim is to check whether a post-WMAP cosmology with dark matter dominating baryons and $h_0 \sim 0.71$ is consistent with several independent stringent observational constraints of the quadruple PG 1115: the image positions, time delays and the mean velocity dispersion of the lens. Our main finding is that the lens models are non-unique: although the constraints are very tight near the Einstein ring, the monopole degeneracy allows the lensing data to be fit by halos with a wide range of profiles at very large and very small radii, from isothermal to constant M/L. This degeneracy may soften the often seemingly conflicting constraints of the lenses. This degeneracy is breakable statistically to some extent by dynamical data and weak lensing data. More data generally helps, e.g., velocity dispersion data. A physical prior (such as equilibrium and positivity) can also help to eliminate some unphysical mass model. However, some level of nonuniqueness always exists because the coverage of the lensing data is patchy, and certain regions of the lens is always underconstrained.

Rusin, Kochanek & Keeton (2003) showed that power-law-like lens models give satisfactory fit to image positions of known lenses. They derive a best-fit lens, which is nearly isothermal with $\alpha \sim 1.07 \pm 0.13$ and $h_0 \sim 0.55 - 0.60$. Here we model the lens galaxy with nearly power-law mass distribution, but the power-law index is allowed to vary with the radius. Unlike Rusin et al. (2003) we do not derive h_0 from the lensing data, instead we use the prior that h_0 is at the post-WMAP value ~ 0.71 to constrain the lens power-law slope α. One powerful way of exploring degeneracies is the pixelated numerical lens model of Saha & Williams (2001, 2004). It is very effective in showing degeneracies due to lenses of different shapes or shear. So far as we know, the consequences and importance of the monopole degeneracy have not been clearly demonstrated in the literature.

2 MASS-SHEET DEGENERACY BROKEN BY POST-WMAP H_0

Consider fitting a general multi-imaged system with the background quasar images at radii $R_i = \sqrt{X_i^2 + Y_i^2}$ from the lens center, where $i = 1, 2$ for double-imaged system and $i = 1, 2, 3, 4$ for quadruple imaged system. The images lie at the extremum points of the time arrival surface following the Fermat principle. The background host galaxy of the quasar is also bent into an Einstein ring, connecting the images. The deflection strength of the lens at any point (X, Y) on the lens plane can be modeled by taking derivatives of a lensing potential $\phi(X, Y)$ with respect to the coordinates (X, Y). The lensing potential is proportional to the non-geometrical part of the time arrival surface.

As a specific example, we consider PG 1115+080, which is a quadruple system with a nearly axisymmetric stellar lens at $z_l = 0.31$, and the quasar source is at $z_s = 1.72$. PG 1115 is the most suitable system even though there are many two-imaged systems with observed time delay and many four-imaged systems with well-constrained lens and image positions but no time delay (e.g., Kochanek 2002a). The lens profile for a two-imaged system has too much freedom, and we really need quadruple systems with time delays and simple (isolated symmetrical lens galaxy) configurations for a meaningful consistency study of the lens profile and h_0. The stellar lens of PG 1115 is well-approximated by a de Vaucouleur profile with a half-light radius of $R_e = 0.75''$ (Treu & Koopmans 2002). We use the photometric data of Treu & Koopmans (2002) for the images A_1, A_2, B, C, and the time delay $t_{BC} = 25 \pm 1.7$ days between the nearest B image and the furthest C image (Schechter et al. 1997). There is an infrared Einstein ring of radius $R_{\rm E} = (0.9 - 1.5)'' = (1.2 - 2)R_e$ passing and surrounding the four images. We adopt a ΛCDM cosmology with $\Omega = 1 - \Lambda = 0.3$ and a post-WMAP H_0,

$$H_0 = 100 h_{\rm WMAP} \sim 71\,{\rm km\ s^{-1}\ Mpc^{-1}}. \tag{1}$$

Like most multi-imaged lens systems, PG 1115 can be fitted by a simple axisymmetrical power-law model for the stellar and dark matter, plus a linear external shear. The amplitudes of the power-law component and the shear component can be determined from the image geometry. The power-law slope is determined by the input value of H_0 and the observed time delay. A power-law profile has a projected density $\kappa_\alpha(R)$ (convergence) and lensing potential $\phi_\alpha(R)$ given by

$$\phi_\alpha(R) = \alpha^{-1} R_{\rm E}^2 \left(\frac{R}{R_{\rm E}}\right)^\alpha, \qquad \kappa_\alpha(R) = \frac{d}{2RdR}\frac{Rd\phi_\alpha(R)}{dR} = \frac{\alpha}{2}\left(\frac{R}{R_{\rm E}}\right)^{\alpha-2}, \tag{2}$$

where $R_{\rm E}$ is the Einstein radius, and the enclosed lens mass $M_\alpha(R)$ is given by

$$M_\alpha(R) \propto 2\int \kappa_\alpha(R) R dR = R^2 \kappa_\alpha(< R) = R_{\rm E}^2 \left(\frac{R}{R_{\rm E}}\right)^\alpha, \tag{3}$$

where $\kappa_\alpha(< R)$ is the average convergence inside the projected radius R. Note the average convergence inside Einstein radius $\kappa_\alpha(< R_{\rm E})$ is unity by definition.

PG 1115 is a member of a group of about 12 bright galaxies (Tonry 1998). For the shear we compute the lensing potential of the other 11 galaxies

$$\phi_{\rm sh}(X, Y) = \sum_{i=1}^{11} \frac{\gamma_i f_i}{2} \ln\left|(X - X_i)^2 + (Y - Y_i)^2\right|, \tag{4}$$

where f_i is the observed flux of the i-th galaxy, and γ_i is a free variable proportional to the mass-to-light ratio of the i-th galaxy. The image positions and source positions satisfy the following lens equation,

$$X_s = [1 - \kappa(< R)]\, X - \partial_X \phi_{\rm sh}, \qquad Y_s = [1 - \kappa(< R)]\, Y - \partial_Y \phi_{\rm sh}, \tag{5}$$

where $R = \sqrt{X^2 + Y^2}$. In total we have 15 free fitting parameters, with (X_s, Y_s) the coordinates of the source, and $(R_{\rm E}, \alpha, \gamma_1, ..., \gamma_{11})$ for the lens model. Since a quadruple system provides in general eight constraints from the image positions, and two or three measurements of relative time delay, the fit to data is therefore underconstrained. To guard against spurious noisy solutions, we minimize the variations of the mass-to-light ratio γ_i among the group members. A few models are shown by the time delay contours in Figure 1a. The image positions are reproduced within 10 milliarcsec.

A nice property of power-law model is that at the Einstein radius

$$\kappa_\alpha(R_{\rm E}) = \frac{\alpha}{2}, \qquad \kappa_\alpha(< R_{\rm E}) = 1. \tag{6}$$

It is a well-known result (e.g., Kochanek 2003; Wucknitz 2002; Zhao & Pronk 2001) that the dimensionless time delay

$$H_0 \Delta t \propto 1 - \kappa_\alpha(R_{\rm E}) = \frac{2 - \alpha}{2}, \tag{7}$$

where the proportionality constant is determined by the image separation and the redshifts of the lens and the source. From the observed time delay $t_{BC} = 25 \pm 1.7$ days between images B and C

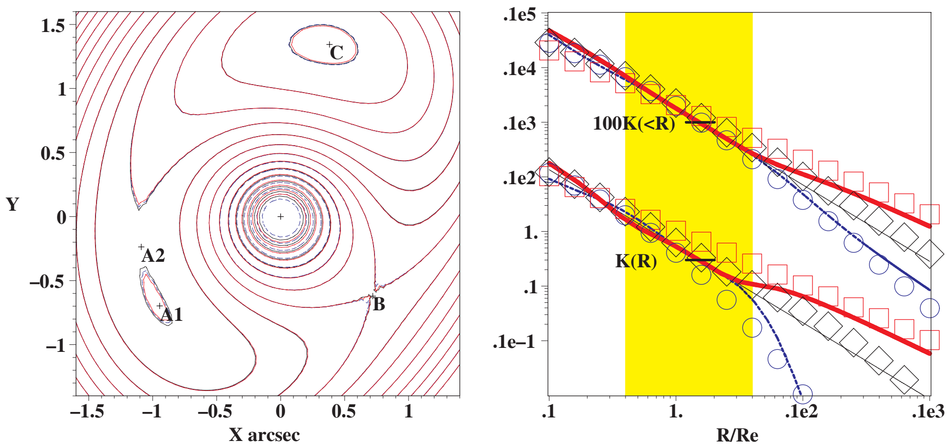

Fig. 1 **(panel a)** Time arrival contours at intervals of 4 days of three different lens models, whose differences are small in time arrival contours, but visible at very inside and very outside of the Einstein ring. They reproduce the same image positions and time delay $t_{BC} = 25 \pm 1.7$ day and the time delay ratio $t_{AC}/t_{BA} = 1.13 \pm 0.18$ (Barkana 1997). **(panel b)** Very different surface density profiles for these lens models, where the convergence $\kappa(R)$ and its average $\kappa(< R)$ (multiplied by 100) are plotted as functions of the rescaled angular radius R/R_e, where R_e is the half light radius of the lens. The middle curve (thin black line) is a model with a simple steeper than isothermal power-law ($\alpha_\infty = \alpha = \alpha_0 = 0.6$), the upper curve (thick red line) is a model with nearly constant circular velocity $u = 220\sqrt{3}\,\mathrm{km\,s^{-1}}$ at large and small radii ($\alpha_\infty = 0.9$, $\alpha_0 = 0.8$), and the lower curve (thin dashed blue line) is a model with a sharply falling density profile ($\alpha_\infty = 0.4$, $\alpha_0 = 0.5$). The shaded zones are typical strong lensing zones $0.4R_e < R < 4R_e$. The predicted dynamical density using de Vaucouleur law assuming self-gravity (circles), imbedded in an NFW halo (diamonds), and using the singular isothermal law (boxes), all normalized by the overall velocity dispersion $220 \pm 20\,\mathrm{km\,s^{-1}}$. All models adopt the post-WMAP cosmology with $H_0 = 71\,\mathrm{km\ s^{-1}\ Mpc^{-1}}$.

and the post-WMAP H_0 we can determine the slope of the power-law lens.[1] We find models with $\alpha = 0.45 - 0.65$ give acceptable fits. This is consistent with Treu & Koopmans (2002) who find a best-fit halo model has a steep volume density cusp $3 - \alpha = 2.35 \pm 0.15$ based on the kinematics and lensing data of PG 1115. Hereafter we adopt the value $\alpha = 0.6$.

Our power-law model has a steeper-than-isothermal density profile, hence a falling circular velocity curve. Interestingly the mass density profile falls off more gradually than the constant M/L de Vaucouleur model (see Fig. 1b), suggesting a moderate increase of M/L, or moderate amount of dark matter at large radii (Fig. 1b). There is very little room to add a much larger amount of dark matter via the mass-sheet degeneracy (i.e., by lowering α), since we must keep the H_0 value within the 4% error bar of the post-WMAP values, and the error of the time delay is only 10%. So in agreement with Kochanek (2003), we also find models with moderately increasing mass-to-light ratio (which have a non-flat circular velocity curve) are sufficient to reproduce the image positions and the "high" value of the Hubble constant.

2.1 Flatten Rotation Curves with Monopole Degeneracy

While the mass-sheet degeneracy is broken by the post-WMAP H_0 and the measurements of time delay, there is still the monopole degeneracy to worry about. The monopole degeneracy maps a lens model to another lens model with very different radial mass distribution but exactly the same

[1] In general, a higher value for the H_0 requires a smaller convergence κ at the Einstein radius, thus a steeper density profile (bigger $2 - \alpha$). For example, varying H_0 from 50 to 100 would change the prediction from an isothermal model to a point mass model.

predicted image positions. Here we are interested in transforming a model with steep falling density and Keplerian circular velocity curves to another model with a large halo and flattish circular velocity curve. Gauss' theorem in a 2-d space guarantees that we can add or remove any amount of mass axisymmetrically outside the Einstein ring without perturbing the images (Schneider et al. 1992). So in principle one has no information of the existence of the outer halo from the inner images. In practice, there are additional physical constraints on the added component. For example, it should keep the overall density positive, smooth and monotonic everywhere. It must not create extra images either. This means that any added halo component must *gently* increase from zero near the images to a significant mass at large radii.

One way of constructing such models is to vary the power-law slope slowly with radius outwards and/or inwards of the Einstein ring. For example, build a new lens potential

$$\phi_u(R) = \phi_\alpha(R)\left[\frac{\phi_{1,u}(R)}{\phi_\alpha(R)}\right]^{\frac{p(R)-\alpha}{1-\alpha}}, \qquad \phi_{1,u}(R) = \frac{2\pi D_{ls} u^2 R}{D_s c^2}, \tag{8}$$

which is a weighted geometric average of the original potential $\phi_\alpha(R)$ (Eq. (2)) and an isothermal potential $\phi_{1,u}(R)$ with a circular velocity u. The new model behaves like a power-law model with

$$\phi_u(R) \propto R^{p(R)}, \tag{9}$$

except that the power-law slope p is a slow-varying function of the radius R. We require $p(R) \sim \alpha$ in the Einstein ring region, so that the new model $\phi_u(R)$ matches almost exactly the old model $\phi_\alpha(R)$ near the images. In the Appendix we give several plausible choices for $p(R)$. One plausible choice for the power-law slope $p(R)$ is

$$p(R) = \alpha + \frac{(x-1)^8}{(\alpha_\infty - \alpha)^{-1} + (\alpha_0 - \alpha)^{-1} x^8}, \qquad x = \frac{R}{1.5 R_e}, \tag{10}$$

which is a U-shaped function of R with the node at a radius 1.5 times the half-light radius R_e, a typical value for the Einstein radius of quadruple lenses. The strong lensing images are typically within a radius range $0.4R_e \le R \le 4R_e$ (e.g., Rusin et al. 2003). As a result, our final model ϕ_u behaves like power-laws at large and small radii with the power slope α_∞ and α_0. However, in the vicinity of the quadruple image radii R_i, we have

$$p(R) - \alpha \sim \pm 0.01, \qquad 0.4R_e \le R \le 4R_e, \tag{11}$$

thanks to the power of eight dependence in Equation (10).

The main effect of replacing $\phi_\alpha(R)$ with $\phi_u(R)$ by the monopole degeneracy is that the lens density profile at very large radii and very small radii is now strongly modified. Models with $\alpha_\infty \sim \alpha_0 \sim 1$ behave like a singular isothermal halo with the deflection power $\frac{d\phi_u(R)}{dR} \to \frac{d\phi_{1,u}(R)}{dR} = cst \cdot u^2$ at large and small radii, hence the circular velocity curve is constant asymptotically with a circular velocity u. Unless specified otherwise, we set $\alpha_\infty = 0.9$ and $\alpha_0 = 0.7$, which yield nearly isothermal models.

A nice property of our new model $\phi_u(R)$ is that its arrival time contours (see Fig. 1a) are almost indistinguishable from the old lens model $\phi_\alpha(R)$ near the images. This means that both models have almost the same light-deflecting power in the region of interest, hence fit the observed image positions and time delays with *almost* exactly the same accuracy; it is possible to make the degeneracy *exact* by choosing an appropriate function for the slope $p(R)$ but the expression is somewhat lengthy (see Appendix). The image positions are reproduced to 10 mas accuracy. All models predict the time delays $t_{AC} = 12.5$ d and $t_{BA} = 11.9$ d, in excellent agreement with the observation results $t_{BC} = 25 \pm 1.7$ days (Schechter et al. 1997), and $\frac{t_{AC}}{t_{BA}} = 1.13 \pm 0.18$ (Barkana 1997).

The new and old lens models have also almost the same light focusing power (related to the curvature of the time arrival surface), hence produce nearly the same amplification map in the Einstein ring region. Varying u from 0 to a few hundred $\mathrm{km\,s^{-1}}$ makes only less than 0.01

magnitude changes in the amplifications because the shear and convergence are barely perturbed near the images. The predicted magnification ratios for the four images are

$$A_1 : A_2 : B : C = 3.2 : -3.6 : -0.61 : 1, \tag{12}$$

where images A_2 and B are saddle points, image C is a minima, and image A_1 a maxima. These are in good agreement with the observed infrared flux ratios

$$A_1 : A_2 : B : C = 3.8 : 2.6 : 0.64 : 1, \tag{13}$$

apart from the well-known problematic flux ratio between the close pair A_1 and A_2. These two close pairs near critical amplification should have nearly the same flux unless the lensing potential is significantly grainy, e.g., due to either microlensing or lensing by substructures (e.g., Impey et al. 1998; Barkana 1997; Metcalf & Zhao 2002) or a wiggle in density profile near the images A_1 and A_2 (which is in principle possible for extreme choices of $p(R)$ and u).

In short, we have a whole sequence of lensing-data-degenerate models with a free parameter u. In fact, we are not restricted to an isothermal model, because the asymptotic power-law slopes α_∞ and α_0 are also changeable. A model with $\alpha_\infty = 0.4, \alpha_0 = 0.5$ is also shown in Figure 1, which resembles a de Vaucouleur model. In general the final density $\kappa_u(R)$ is smooth, monotonically decreasing and positive everywhere (see Fig. 1b). The lens density model is not only mathematically positive and smooth but also does not create extra images.

Note that the monopole degeneracies do not affect the determination of H_0, because they do not perturb the lens potential near the images, but they taper the mass distribution at small and large radii to fit any central velocity dispersion of the lens and any weak shear at large radii. This is very different from the mass-sheet degeneracy, which is well-constrained by the H_0 value determined by lensing-independent observations.

2.2 Compare Strong Lensing with Dynamics and Weak Lensing of Ellipticals

The circular velocity curve in ellipticals can be constrained from the stellar velocity dispersions. It is generally a difficult task to carry out a reliable measurement of the dispersion profile for a faint lens surrounded by four bright quasar images. Nevertheless, Tonry (1998) measured a dispersion of $281 \pm 25\,\mathrm{km\,s^{-1}}$ of PG 1115 in an 1-arcsec aperture under 0.8 arcsec seeing. This is effectively the mean 1-dimensional velocity dispersion of the perhaps spherical stellar component of the galaxy. Apply this dispersion in the virial theorem we can normalise the overall mass distribution in the lens galaxy. Assuming the lens galaxy potential has a flat rotation curve V_{cir}, then stars inside should have a mean dispersion $\sigma_{\mathrm{obs}} = V_{\mathrm{cir}}/\sqrt{3}$. For a self-gravitating de Vaucouleur model the effective rms velocity is $\sqrt{\frac{GM_{dV}}{R_e \sigma^2_{\mathrm{obs}}}} \sim 3.0$, where M_{dV} is the total mass. Note that Tonry's measurement is subject to possible contamination of the quasar light. However, the dispersion $\sigma_{\mathrm{obs}} \sim 281\,\mathrm{km\,s^{-1}}$ is surprisingly high as noted in Tonry (1998). If PG 1115 were a typical L_* elliptical galaxy on the fundamental plane, it should have a dispersion $\sim 180\,\mathrm{km\,s^{-1}}$ (Treu & Koopmans 2003). Tonry's dispersion of PG 1115 is nearly as big as the dispersion $\sim 270 \pm 70\,\mathrm{km\,s^{-1}}$ of the galaxy group, which means that the other members of the group are within the gravitational influence of or nearly bound to PG 1115, which is clearly not the case. The center of light is in fact near the brightest group member (G1) 20 arcsec away. Perhaps a more reliable estimate for PG 1115's dispersion is to rescale the dispersion of G1 with the Faber-Jackson relation given that PG 1115 is a scaled-down version of G1, and G1's measurement is presumably reliable and free from problems of contamination from the quasar images. G1 is about 1.8 times as luminous as PG 1115, so if we take Tonry's dispersion for G1 $256 \pm 20\,\mathrm{km\,s^{-1}}$, and scale down by a factor $1.8^{-0.25}$, we have $220\,\mathrm{km\,s^{-1}}$ for the dispersion of PG 1115. Hereafter we take $\sigma_{\mathrm{obs}} = 220 \pm 20\,\mathrm{km\,s^{-1}}$ as a conservative estimate of the dispersion of PG 1115.

The mass profile of the lens mass is very model dependent, and there is no direct dynamical measurement. Still one can use either CDM simulations or the ellipticals in the local universe as templates to the expected circular velocity profile. Based on a sample of 21 nearby ellipticals, Gerhard et al. (2001) suggested that the circular velocity curves in ellipticals are *consistent* with being nearly flat (only 10% variation) in the inner two effective radii. This suggests a model for L^* ellipticals with a large halo of a characteristic circular velocity $\sim 250\,\mathrm{km\,s^{-1}}$ dominating at large radii, a picture which is also consistent with satellite galaxy dynamics, X-ray density and temperature profiles, and weak lensing of ellipticals (Prada et al. 2003; Lowenstein & White 1999; Guzik & Seljak 2002). However, a recent study of PNs in three ellipticals by Romanowsky et al. (2003) found a rapidly falling velocity dispersion at five effective radii, consistent with a constant M/L de Vaucouleur model, suggesting a model with nearly Keplerian star-dominated mass distribution at large radii.

The CDM halos are not rigorously isothermal. In these models an elliptical galaxy roughly consisted of a de Vaucouleur model imbedded in an NFW halo, if we assume the opposing effects of adiabatic contraction and dynamical feedback due to the baryonic component cancel each other. A typical (or M^*) NFW halo has a virial velocity $V_{\rm vir} \sim 200\,\mathrm{km\,s^{-1}}$, a virial radius about 10 core radii, and a mass of about 10 times the baryonic component. If we superimpose such an NFW halo on our baryon-only model (de Vaucouleur model), we obtain a model density profile (diamonds) intermediate between isothermal (boxes) and de Vaucouleur model (circles), as shown in Figure 1b.

Comparing the dynamical model with the lens models shows some interesting results. The pure power-law lens model (thin black line) with $u = 0$ resembles the CDM dynamical models but with somewhat lower dark matter content, the lens model with $\alpha_\infty = 0.9$ and $\alpha_0 = 0.8$ (thick red line) resembles the isothermal dynamical model at small and large radii, and the lens model with a steep slope $\alpha_\infty = 0.4$, $\alpha_0 = 0.5$ (thin dashed blue line) resembles the constant M/L de Vaucouleur dynamical model. These results apply to both the density (see Fig. 1b) and the average density (see Fig. 1b). One can compute the logarithmic slope of the mass profile $\alpha(R) = \frac{d\log M}{d\log R}$. All models are between a uniform mass-sheet $\alpha = 2$ and Keplerian ($\alpha \sim 0$), and they have the same slope $\alpha = 0.6$ at the strong lensing zone.

It might appear surprising that both lens models with and without a large cuspy halo can be made consistent with the lensing position, the time delay data and the post-WMAP H_0. It shows the flexibility of the monopole degeneracy. We do not find a conflict between lens models with a large dark halo and the post-WMAP H_0. Neither do we find a conflict between the mass profile of the lenses and the dynamical mass profile of nearby ellipticals given the uncertainties of the dynamical models. Instead we find that the new mass degeneracy prevents us from drawing a robust conclusion about the dark halo on the basis of the image positions and time delays alone.

3 DISCUSSION

Here we have demonstrated a specific way to construct non-unique models for fitting the same strong lensing data, including time delays. We lift the well-known mass-sheet degeneracy by hard-wiring the H_0 to the post-WMAP value. We build models with positive, smooth and monotonic surface densities. We find the strong lens data of PG 1115 can be explained to the same accuracy by models with nearly constant M/L and by models with nearly flat circular velocity curve; the latter models are preferred only when galaxy-galaxy weak lensing shear at large radii is considered. The ambiguity is further compounded by the surprising kinematics of PNs at five effective radii in a few L_* elliptical galaxies (Romanosky et al. 2003), which does not confirm the expectation of a flat circular velocity curves as suggested by earlier studies of a larger sample with velocity data within about two effective radii (Gerhard et al. 2001). The models shown in Figure 1b are consistent with velocity dispersion profile ranging from nearly flat (isothermal, red thick curve vs. box symbols) to steeply falling (blue dashed curve vs. circles). This shows the range of degeneracy in modeling the lens.

It is difficult to say whether PG 1115 is a representative case for strong lenses, and to what extent we can generalize our conclusions here. PG 1115 appears to be an unremarkable L_* E0 galaxy. It is one of the quadruple time delay systems with the simplest geometry and maximum lensing constraints. These properties might have made it too good for modelling to be representative, but still the data are not good enough to remove the monopole degeneracy, and one has to rely on statistical arguments based on the flatness of circular velocity curves from dynamics and weak lensing of nearby ellipticals of comparable luminosity. In an extensive review on known degeneracies in the mass modelling of strong lenses by Saha (2000), there is only a brief mentioning of monopole degeneracy as a mathematically trivial point.

Parametric models in the literature typically make use of only a narrow class of smooth profiles, e.g., NFW profile, or more generally the double power-law halo profiles in Zhao (1996). However, in principle the halo densities could have been compressed or depressed at a few effective radii due to dynamical feedbacks from the baryonic component. One can derive less model-dependent information about the lens if one uses a looser parametrization for the density models, as is done here using power-law model with a slow-varying slope.

Nevertheless, the drawback of our proposed density models for PG 1115 is that these models are somewhat contrived. While they are not obviously unphysical given their positive densities everywhere, and their mathematical details cannot yet be linked to real physical processes in galaxy formation. It is not obvious how to fix this obvious drawback of our halo model while *still keeping the lensing model analytical*, which is the spirit of this paper in addressing the apparent conflict of lensing data with CDM cosmological parameters. A study from a different angle is perhaps needed.

In short, it seems safe to conclude on a few general points: (i) The significance of the mathematically-trivial monopole degeneracy has not been well appreciated before, particularly its role in softening the H_0 vs time delay crisis. (ii) Deriving the halo inner and outer profiles from lensing generally involves an unreliable extrapolation from a measurement of power-law slope at the Einstein ring. (iii) Hardwiring the H_0 breaks the mass-sheet degeneracy of lenses, and observed time delays yield a slope $\frac{d\log M}{d\log R} \sim 2(1-h_0) \sim 0.6$, significantly below isothermal at about 1.5 effective radii if the post-WMAP $h_0 \sim 0.7$ is taken. (iv) Spatially well-resolved dynamical data in the inner five effective radii in high redshift lenses or their local template ellpticals are in urgent need for breaking the monopole degeneracy in lenses, and constraining the nature of the dark matter.

4 LENSING IN RECENT RELATIVISTIC VERSION OF MODIFIED NEWTONIAN DYNAMICS

Finally, we note that dark matter models are not the only models for galaxies, and there have been a revival of interests in modified gravity recently. In particular the MOND theory by Milgrom (1983) explains galaxy circular velocity curves very well (Sanders & McGaugh 2002), in particular, they could explain the velocity dispersion profiles of low-redshift elliptical galaxies (Milgrom & Sanders 2003), in particular the recent PNe data (Romanowsky et al. 2003). MOND predicts slightly falling velocity dispersion curves out to five effective radii for high surface brightness ellipticals, and it becomes flat at larger radii. In these models, there is no dark matter, but gravity from the baryonic matter is modified from Newtonian or General Relativity (GR). The non-relativisitic MOND theory has gained a relativistic counterpart recently, called TeVeS. It passes standard local and cosmological tests used to check GR (Bekenstein 2004). The TeVeS theory is so named because it contains a conformal GR-like metric tensor, one new vector field, two new scalar fields to preserve general covariance. Following Bekenstein (2004), a number of other works have appeared studying galaxy dynamics (Ciotti & Binney 2004; Baumgardt et al. 2005; Read & Moore 2005), galaxy cluster dynamics (Pointecouteau & Silk 2005), cosmological model (Hao & Akhoury 2005), and large-scale structure of the universe (Skordis et al. 2005) in the relativistic TeVeS. Here we comment on its application to the gravitational time delay in PG 1115.

It is becoming possible to predict lensing in the MOND theory (Qin et al. 1995; Chiu et al. 2005; Zhao et al. 2005). Interestingly, the bending angle in TeVeS or MOND has the standard form as in GR. The only difference is that the lens gravitational potential is related to the baryonic matter distribution by a modified Poisson's equation with an effective dielectric constant depending on the strength of the gravity. In fact, the bending angle is uncunningly the same as presented in Qin et al. (1995). For a light path with impact parameter $b = D_l\theta$ from a spherical lens, the bending angle (cf. equation in the abstract of Qin et al. and eq. (109) of Bekenstein)

$$\alpha = \int_{-\infty}^{\infty} 2g_\perp \frac{dx}{c^2}, \qquad g_\perp = \frac{D_l\theta}{r} g(r), \qquad x = \sqrt{r^2 - (D_l\theta)^2}, \tag{14}$$

where we integrate the perpendicular impulse along the line of sight length x, the factor of two is due to relativity, and $g_\perp$ is the perpendicular component of the gravity $g(r)$ at radius r from the spherical lens galaxy. The MONDian gravitational field around a spherical stellar distribution of the total mass M_* is given by

$$g = \begin{cases} g_N = \frac{GM_*}{r^2} \gg a_0 \sim 1 \times 10^{-8} \mathrm{cm\,s^{-2}} & r \gg r_0, \\ \sqrt{g_N a_0} = \frac{v_0^2}{r} & r \ll r_0, \end{cases} \tag{15}$$

where

$$r_0 = \sqrt{\frac{GM_*}{a_0}},\ v_0 = (GM_* a_0)^{1/4}, \tag{16}$$

are the radius of the so-called "Newtonian bubble", and the asymptotic circular velocity. As a result a test particle well outside the Newtonian bubble will reach a flat circular velocity curve of $V_{\rm circ}(r) = v_0 \propto M_*^{1/4}$. This is the main reason behind the MOND's success, i.e., why rotation curves of spiral galaxies are flat and satisfy the Tully-Fisher relation $L \propto v_0^4$. We refer the interested readers to Zhao et al. (2005) for an overview of dynamics, cosmology and lensing in MOND/TeVeS.

For PG 1115 at $z_l = 0.3$ the lens has an I-band magnitude of $I = 18.92$. Assume a baryonic open cosmology with a cosmological constant term as in Zhao et al. (2005), and use a Hubble constant of $h_0 = 0.7$, we find

$$D_l = 0.88\,\mathrm{Gpc},\ D_s = 1.7\,\mathrm{Gpc},\ D_{ls} = 1.2\,\mathrm{Gpc},\ \frac{D_{ls} D_l}{D_s} = 0.65\,\mathrm{Gpc} = 0.65 \times 10^{12} \text{ light days}. \tag{17}$$

For an old single burst model for the early-type lens the K-correction and evolution correction cancel approximately in I-band at intermediate redshift, and the mass-to-light at the restframe I-band is about $M/L = 4$. So the stellar mass of the lens is found to be (Zhao et al. 2005)

$$M_* = 10^{11}\ \mathrm{M}_\odot, \tag{18}$$

which is typical for an L_* galaxy. If we take the standard value for a_0, MOND would predict an asymptotic circular velocity for the galaxy

$$V_{\rm circ}(\gg r_0) = (GM_* a_0)^{1/4} = 200\,\mathrm{km\,s^{-1}}, \qquad r_0 \equiv \sqrt{\frac{GM_*}{a_0}} = 12 \text{ kpc}. \tag{19}$$

Observationally the images are near the Einstein ring $R_{\rm E} = 1'' = 4.4$ kpc, and inside it the average velocity dispersion is $\sigma_{\rm obs} = 281 \pm 25\,\mathrm{km\,s^{-1}}$ (Tonry 1998). The fact that $r_0 > R_{\rm E}$ and $V_{\rm circ} < \sigma_{\rm obs}$ suggest two interesting points.

(i) The asymptotic circular velocity appears too low compared to the observed dispersions. Considering that the observational error might be underestimated given very bright quasar images within $0.5''$ of the lens galaxy, it is helpful to have an indirect measurement. Now, PG 1115 belongs to the same group as G1, and G1 is the brightest group member (1.8 times as luminous as PG 1115) and has a measured dispersion $256 \pm 20\,\mathrm{km\,s^{-1}}$ by Tonry. If we scale down $256\,\mathrm{km\,s^{-1}}$ by a factor $1.8^{-0.25}$ according to the Faber-Jackson relation, we have $220\,\mathrm{km\,s^{-1}}$ for the dispersion of PG 1115, which is barely consistent with what MOND predicts. A larger a_0 or M_* could help to improve the fit. A cautionary note: the terminal circular velocity is non-trivially related to the central velocity dispersion by the Jeans equation in MOND. MOND predicts slightly falling velocity dispersion curves out to five effective radii for high surface brightness ellipticals, and it becomes flat at larger radii. Although for many models one expects a central dispersion lower than the terminal circular velocity, the prediction is not unique depending on the velocity anisotropy and baryonic mass profile (Sanders & Milgrom 2003).

(ii) All images on the Einstein ring must have a path intersecting with the "Newtonian bubble". As a light ray goes from infinity to the lens and then to the observer, the gravity increases from very weak to some significant value and then drops to nearly zero again. For a light path with a large impact parameter b, the gravity could be weak all the way (see solid light path, Fig. 2). This,

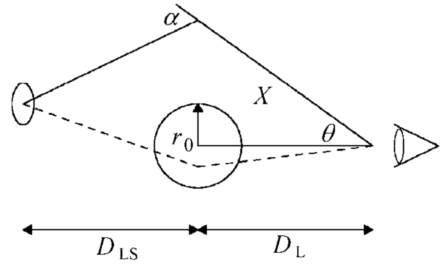

Fig. 2 A schematics of bending of light. The radius $r_0 = \sqrt{\frac{GM_*}{a_0}}$ is the radius outside which the gravity of a galaxy of stellar mass M_* is weaker than the critical value of $a_0 \sim 10^{-8}\mathrm{cm\,s^{-2}}$; generally $r_0 \sim 10\,\mathrm{kpc}$ for L_* galaxies, such as the lens galaxy PG 1115. The Einstein rings and the images of most lenses all lie within the radius r_0 (in fact the images are at about 1-2 times the effective radius $R_e \sim 3\,\mathrm{kpc}$), hence at the image positions the gravity is in the strong regime.

however, is not the case for many lensed images. As also found by Zhao et al. (2005), the ray must always cross the strong gravity regime for a duration of

$$\frac{x_0}{c} = \frac{\sqrt{r_0^2 - R_i^2}}{c} \sim \frac{11\ \mathrm{kpc}}{\mathrm{c}} \sim 10^7\ \mathrm{days}, \tag{20}$$

where R_i is the image separation from the lens in the lens plane, the innermost and outermost images B and C of PG 1115 are at $R_i = 0.8'' = 3.5\,\mathrm{kpc}$ and $R_i = 1.6'' = 7\,\mathrm{kpc}$, respectively. During this 10^7 days the space-time metric is slightly curved, and can be written in rectangular coordinates as

$$-c^2 d\tau^2 = -\left(1 + \frac{2\Phi}{c^2}\right) d\tilde{t}^2 + \left(1 - \frac{2\Phi}{c^2}\right)(dx^2 + dy^2 + dz^2),\ \Phi(r) \approx -\frac{GM_*}{r}\,, \tag{21}$$

where $\Phi(r)$ is the gravitational potential of the Newtonian dynamics. This potential creates a so-called Shapiro time delay Δt_{Shap}. Since we are in the strong gravity regime, GR applies without any modification, hence we can use the usual expression for time delay

$$\Delta t_{\mathrm{Shap}} = -\frac{1+z_l}{c}\int_{-x_0}^{x_0} \frac{2\Phi(r)}{c^2} dx \approx \frac{4(1+z_l)GM_*}{c^3} \ln\left(\frac{r_0}{R_i} + \sqrt{\frac{r_0^2}{R_i^2} - 1}\right), \tag{22}$$

where the factor $(1 + z_l)$ corrects for time dilation. Substitute in the positions of images B and C we find the relative Shapiro delay $\Delta t^{BC}_{\mathrm{Shap}} = 21$ days. A similar calculation can be done for the segments of the light path in the weak regime using a modified potential. Its contribution turns out to be less than 1 day, hence can be neglected. The geometrical time delay can also be calculated in the usual way, and we find $\Delta t^{BC}_{\mathrm{geo}} = 12$ days. So the total delay can be $\Delta t^{BC} = 33$ days. The observed time delay $t^{BC}_{\mathrm{obs}} = 25 \pm 2$ days. This means that a simple application of MOND/TeVeS can explain the observed time delay to a factor of two, and some adjustment of M_* or a_0 or h_0 might be necessary to fit the data on time delay and velocity dispersion exactly.

Acknowledgements We acknowledge helpful comments from Daniel Mortlock, Prasenjit Saha and the anonymous referee. BQ acknowledges hospitality in a visit to the Institute of Astronomy, Cambridge, which started this work. HSZ thanks support from UK PPARC Advanced Fellowship. This work was also supported in part by the National Natural Science Foundation of China (NSFC) under Grants 10428308 to HSZ, 10233040 and 10003002 to BQ.

Appendix A: PLAUSIBLE FUNCTIONAL FORMS FOR THE POWER-LAW INDEX $p\,(R)$

Here are a few examples for $p(R)$ based on slightly different considerations. We can make $p(R)$ a piecewise function of R, so that $p(R) = \alpha$ is constant over the entire Einstein zone.

$$p(R) = \alpha, \qquad 0.4 < \frac{R}{R_e} \leq 4 \tag{A1}$$

$$= \alpha + (\alpha_0 - \alpha)\left(\frac{R}{0.4R_e} - 1\right)^8, \qquad \frac{R}{R_e} < 0.4 \tag{A2}$$

$$= \alpha + (\alpha_\infty - \alpha)\left(\frac{R}{4R_e} - 1\right)^{-8}. \qquad \frac{R}{R_e} > 4 \tag{A3}$$

Or we can make $p(R) = \alpha$ only at the image positions. Let $p(R) = \alpha + w(R)$, and

$$w(R) = \frac{\prod_{i=1}^{i=N}(R - R_i)^2}{R^{2N}(\alpha_\infty - \alpha)^{-1} + (\alpha_0 - \alpha)^{-1}\prod_{i=1}^{i=N} R_i^2}, \tag{A4}$$

which is a smooth wavelike function with N-nodes at images $R_1 ... R_N$, i.e., $w(R_i) = \frac{dw(R_i)}{dR_i} = 0$.

Or we can make $p(R) \sim \alpha$ on the entire strong lensing zone. The expression for it is given in Eq. (10).

Be ware not to confuse $p(R)$ with the mass profile slope $\alpha(R) \equiv \frac{d \log M}{d \log R}$. The two are the same only for simple power-law models.

Appendix B: OTHER WAYS OF CREATING DEGENERACY

A more general model can be built from the following linear decomposition, i.e.,

$$\phi(R) = (1 - \delta_0)\phi_0(R) + \delta_0 U_0(R) + \delta_1 U_1(R) + \delta_2 U_2(R), \tag{B1}$$

where δ's are non-zero coefficients of additional dark components $U(R)$. These are distortions or deviations on top of any dark matter already implied in the constant mass-to-light model. The question here is, what are the allowed functional forms for $U(R)$? More specifically, how can we add a dark halo distortion to the constant mass-to-light model $\phi_0(R)$ with vanishing perturbation to the image positions? First of all, there is the well-known mass-sheet degeneracy. Such a constant density lens component has a potential of the form $\frac{\delta_0}{2}R^2$, where δ is the constant convergence of the mass sheet. Since real galaxy density typically falls sharply at large radii, and has a nearly isothermal cusp at small radii, we should taper the simple mass sheet potential smoothly inwards and the outwards of the Einstein ring. If the images and the Einstein ring are bracketed by an inner radius $R_{\rm in}$ and outer radius $R_{\rm out}$ with

$$R_{\rm in} < R_i < R_{\rm out}, \qquad i = 1, 2, 3, 4, \tag{B2}$$

then one can add, for example, a tapered mass-sheet (dark) component $\Delta\phi_h(R) = \delta_0 U_0(R)$, where

$$U_0(R) = \frac{R^2 - R_{\rm out}^2}{2}, \qquad R_{\rm in} \leq R \leq R_{\rm out} \tag{B3}$$

$$= R_{\rm out}^2 \ln\left(\frac{R^3}{3R_{\rm out}^3} + \frac{2}{3}\right), \qquad R > R_{\rm out} \tag{B4}$$

$$= \left[b_0 + b_1 R^{1+\beta} + b_2 \beta R^{1/\beta}\right]. \qquad R < R_{\rm in} \tag{B5}$$

It is easy to verify that the potential, mass and density are continuous across $R_{\rm out}$. By choosing the coefficients b_0, b_1 and b_2 we can ensure that the potential, mass and density are continuous across $R_{\rm in}$ as well. Note this construction of the halo has a finite mass $3\delta_0 R_{\rm out}^2$ at large radius, and an isothermal density at small radius for $\beta \sim 0$. It is well-known that the image positions are invariant if we decrease the mass-to-light ratio of the $\phi_0(R)$ model by a factor $\eta = 1 - \delta_0$ at the same time (cf. Eq. (B1)). Nevertheless, adding the above component has an effect measurable by time delays. The dimensionless image time delay

$$H_0 \Delta t_{\rm obs} \rightarrow (1 - \delta_0) H_0 \Delta t_{\rm obs}. \tag{B6}$$

Now that H_0 can be well-determined by other distance ladders (e.g., $H_0 = 72 \pm 8$ from the HST Key Project) greatly restricts the leverage of any mass-sheet degeneracy. Are there any other more subtle ways of modifying the constant mass-to-light models? Can we add dark matter in a way by-passing the time-delay and all other strong lensing data? Certainly, there is the monopole degeneracy, which is so simple that it is seldom considered. For example, we can add a large amount of halo mass beyond a radius $R_{\rm out}$ and nothing inside. As long as $R_{\rm out}$ is outside the images and Einstein ring, there would be no effect on the images inside because of the Gauss theorem. The real challenge is to avoid creating unrealistic discontinuity or negative density regions in the galaxy, particularly at the transition region. This is certainly possible, for example, with a potential $\Delta\phi_h(R) = \delta_2 U_2(R)$, where

$$U_2(R) = \frac{R_{\rm out}^2}{2}\left[1+\ln^4\left(\frac{R}{R_{\rm out}}\right)\right]^{\frac{1}{2}} - \frac{R_{\rm out}^2}{2}, \qquad R > R_{\rm out} \tag{B7}$$

$$= 0. \qquad R \le R_{\rm out} \tag{B8}$$

It is easy to verify

$$\Delta\phi_h = 0, \qquad \Delta\phi_h' = 0, \qquad \Delta\phi_h'' = 0, \qquad \text{at } R = R_{\rm out}\,. \tag{B9}$$

This means that this dark component does not contribute to the density and the deflection at $R_{\rm out}$ or within. At large radii, however, the system mass diverges as $\propto \ln(R)$, resembling the CDM models (Navarro et al. 1997). There should not be extra images anywhere unless δ_2 is very big. Since there is no halo inside $R_{\rm out}$, there is no effect on strong lensing. The effect is only in the weak lensing at large radii. What about the inner mass distribution? The same monopole degeneracy allows us to move mass around inside a radius $R_{\rm in}$ without any imprints on strong lensing as long as $R_{\rm in}$ is within all the images and Einstein ring. For example, we can turn some stellar mass into dark matter, the latter can have a potential $\Delta\phi_h(R) = \delta_1 U_1(R)$, where

$$U_1(R) = \left[c_0 + c_1 R^{1+\beta} + c_2\beta R^{1/\beta} - \frac{R_{\rm in}^2}{\alpha}\ln\left(1+\frac{R^\alpha}{R_e^\alpha}\right)\right], \qquad R < R_{\rm in} \tag{B10}$$

$$= 0, \qquad R \ge R_{\rm in} \tag{B11}$$

where the constants c_0, c_1 and c_2 must satisfy the implicit relation

$$\Delta\phi_h(R_{\rm in}) = 0, \qquad \Delta\phi_h'(R_{\rm in}) = 0, \qquad \Delta\phi_h''(R_{\rm in}) = 0. \tag{B12}$$

These fix the exact expressions for the coefficients c_i. Effectively this halo component has no net mass and density at radius $R_{\rm in}$ and outside, hence it does not influence the images because of Gauss theorem. By adjusting the amplitude $0 \le \delta_1 \le 1$ and the power-law slope $\beta \sim 0$, however, we can modify the inner rotation curve to a flat rotation curve, or whatever the observations require. We choose the value of α such that the stellar distribution has a cusp slope $2-\alpha$; here we choose $2-\alpha = 0$ for the $R^{1/4}$-law since this profile has no projected cusp. In short, we have shown a specific way to construct non-unique models for fitting the same strong lensing data. [2] In particular, the component $\delta_1 U_1(R) + \delta_2 U_2(R)$ can keep the convergence κ, shear γ, the components of the amplification matrix μ and the time delay between images unchanged at the radii of the (e.g., four) images $R = R_i$. In fact it has a vanishing contribution to *the arrival time surface near the images*. The only dynamical effect is that they modify the rotation curve of the lens galaxy. Thus we have found a general method to separate the observational constraints of strong lensing from constraints of galaxy dynamics. Together with a adjustable tapered mass-sheet component, we can create mass models of various rotation curves consistent with the lensing data. The time delay surface is

$$\begin{aligned}\tau(X,Y) &= \frac{(X-X_{s,0}\eta)^2 + (Y-Y_{s,0}\eta)^2}{2} \\ &- \frac{\eta\gamma_1(X^2-Y^2) + 2\eta\gamma_2 XY}{2} \\ &- \frac{\eta m_0}{\alpha}\ln\left(1+\frac{R^\alpha}{R_e^\alpha}\right) \\ &- \eta U_0(R) - \delta_1 U_1(R) - \delta_2 U_2(R).\end{aligned} \tag{B13}$$

Hence when we vary the parameter δ_1 and δ_2 the time arrival surface $\tau(X,Y)$ yields the same extrema, or images. This means models with different halo will have goodness of fit to all strong lensing data (the time delay, the image positions and even the amplifications and parity of the images). It only alters the mass distribution of the lens, e.g., the total mass of the lens and the spatial extent of the lens. Hence it creates a degeneracy in lens modeling, making it problematic to draw unique conclusions on lens halo mass from image modeling.

[2] In an earlier preprint, we also show a way to construct a halo with non-zero density everywhere except at the images.

References

Barkana R., 1997, ApJ, 489, 21
Bartelmann M., Schneider P., 2001, Phys. Rep., 340, 291
Baumgardt H., Grebel E. K., Kroupa P., 2005, astro-ph/0501272
Bekenstein J., 2004, Phys. Rev. D, 70, 3509
Bekenstein J., Milgrom M., 1984, ApJ, 286, 7
Chen D.-M., 2004a, A&A, 418, 387
Chen D.-M., 2004b, ChJAA, 4, 118
Chiu M. et al., astro-ph/0507332
Ciotti L., Binney, J., 2004, MNRAS, 351, 285
Freedman W. L., Madore B. F., Gibson B. K. et al., 2001, ApJ, 553, 47
Gerhard O., Kronawitter A., Saglia R. P., Bender R., 2001, AJ, 121, 1936
Gorenstein M. V., Shapiro I. I., Falco E. E., 1988, ApJ, 327, 693
Guzik J., Seljak U., 2002, MNRAS, 335, 311
Hao J., Akhoury R., 2005, astro-ph/0504130
Impey C. D., Falco E. E., Kochanek C. S. et al., 1998, ApJ, 509, 551
Kochanek C. S., 2002a, ApJ, 578, 25
Koopmans L., Fassnacht C. D., 1999, ApJ, 527, 513
Koopmans L., Treu T., 2002, MNRAS, 337, 6
Metcalf B., Zhao H., 2002, ApJ, 567, L5
Milgrom M., 1983, ApJ, 270, 365
Milgrom M., Sanders R. H., 2003, ApJ, 599, L25
Pointecouteau E., Silk J., 2005, astro-ph/0505017
Prada F., 2003, ApJ, 598, 260
Qin B., Wu X.-P., Zou Z.-L., 1995, A&A, 296, 264
Romanowsky A. J., Douglas N. G., Arnaboldi M., 2003, Science, 301, 1696
Read J., Moore B., 2005, astro-ph/0501273
Refsdal S., 1964, MNRAS, 128, 307
Rusin D., Kochanek C., Keeton C., 2003, ApJ, 595, 29
Navarro J., Frenk C., White S. D. M., 1997, ApJ, 490, 493
Saha P., 2000, AJ, 120, 1654
Saha P., Williams L. L. R., 2001, AJ, 122, 585
Saha P., Williams L. L. R., 2004, AJ, 127, 2604
Sanders R., McGaugh S., 2002, ARA&A, 40, 263
Schechter P. L. et al., 1997, ApJ, 475, L85
Schneider P., Ehlers J., Falco E. E., 1992, Gravitational Lenses, Berlin: Springer
Skordis C., Mota D. F., Ferreira P. G., Boehm C., 2006, Phy. Rev. Lett., 96, 011301
Spergel D. N., Verde L., Peiris H. V. et al., 2003, ApJS, 148, 175
Tonry J. L., 1998, AJ, 115, 1
Treu T., Koopmans L., 2002, MNRAS, 337, 6
Weinberg D., Katz N., 2002, ApJ, 580, 627
Williams L. L. R., Saha P., 2000, AJ, 119, 439
Wu X.-P., 1996, Fundam. Cosmic Phys., 17, 1
Wucknitz O., 2002, MNRAS, 332, 951
Zhao H. S., 1996, MNRAS, 278, 488
Zhao H. S., Pronk D., 2001, MNRAS, 320, 401
Zhao H. S., Qin B., 2003, ApJ, 582, 2 (Paper I)
Zhao H. S., Bacon D., Taylor A. N., Horne K. D., 2005, MNRAS, submitted (astro-ph/0509590)